

Author(s)	Leeds, Rene W.
Title	Computer simulation studies of copper atoms in 110 channels of copper crystals.
Publisher	Monterey, California. Naval Postgraduate School
Issue Date	1964
URL	http://hdl.handle.net/10945/24640

This document was downloaded on August 03, 2015 at 03:43:19



<http://www.nps.edu/library>

Calhoun is a project of the Dudley Knox Library at NPS, furthering the precepts and goals of open government and government transparency. All information contained herein has been approved for release by the NPS Public Affairs Officer.

**Dudley Knox Library / Naval Postgraduate School
411 Dyer Road / 1 University Circle
Monterey, California USA 93943**



<http://www.nps.edu/>

NPS ARCHIVE
1964
LEEDS, R.

COMPUTER SIMULATION STUDIES OF
COPPER ATOMS IN 110 CHANNELS
OF COPPER CRYSTALS

RENE W. LEEDS

DUDLEY KNOX LIBRARY
NAVAL POSTGRADUATE SCHOOL
MONTEREY CA 93943-5101

LIBRARY
U.S. NAVAL POSTGRADUATE SCHOOL
MONTEREY, CALIFORNIA

COMPUTER SIMULATION STUDIES
OF COPPER ATOMS IN 110 CHANNELS OF COPPER CRYSTALS

* * * * *

RENE W. LEEDS

COMPUTER SIMULATION STUDIES
OF COPPER ATOMS IN 110 CHANNELS OF COPPER CRYSTALS

by

Rene W. Leeds

Lieutenant, United States Navy

Submitted in partial fulfillment of
the requirements for the degree of

MASTER OF SCIENCE
IN
PHYSICS

United States Naval Postgraduate School
Monterey, California
1964

LIBRARY
U.S. NAVAL POSTGRADUATE SCHOOL
MONTEREY, CALIFORNIA

COMPUTER SIMULATION STUDIES

OF COPPER ATOMS IN 110 CHANNELS OF COPPER CRYSTALS

by

Rene W. Leeds

This work is accepted as fulfilling
the thesis requirements for the degree of

MASTER OF SCIENCE

IN

PHYSICS

from the

United States Naval Postgraduate School

ABSTRACT

The interaction of 1 and 5 keV copper atom (primaries) impacting the (111) surface of copper crystals was studied using an "n-body type" computer simulation program. Each primary energy was studied using both the Bohr and Gibson II copper on copper potentials. Primary penetration and lateral drift or spread were investigated as a function of impact point.

The n-body program has greater penetration values than the binary model used by Robinson and Oen¹³. Drift or spread (defined as wander if energy loss rate is low) occurs in the impact region of transition from hard interaction (near a lattice atom) to soft interaction (open or channel regions). Penetration and spread contours are presented.

The guidance and assistance given by Associate Professor Don E. Harrison, Jr. of the U. S. Naval Postgraduate School in this study is gratefully acknowledged.

TABLE OF CONTENTS

Section	Page
1. Introduction	1
2. Computer Simulation Studies	6
3. Objectives	10
4. Simulation Model	11
5. Procedure	18
6. Results and Conclusions.....	24
7. Bibliography	50
Appendix	
I. Program Listing.....	52
II. Program Discussion	61
III. Program Operating Instructions	69

LIST OF ILLUSTRATIONS

Figure	Page
1. Integral Penetration Curves	35
2. Robinson and Oen "... (110_ channel trajectories onto (011) surface for f.c.c. Cu"	36
3. (110) Face of Chan2 Type Crystal	37
4. (110) Face of Chan4 Type Unit Crystal	38
5. N-body Model Trajectories	39
6. Integral Penetration Curves	40
7. Depth of Penetration and Maximum Scatter Correlation Plots	41
8. Impact Triangle, 14 and 12 point grid systems	42
9. Contour Curves. Gibson II potential and 5000ev primaries	43
10. Contour Curves. Gibson II potential and 1000ev primaries	44
11. Contour Curves. Bohr potential and 5000ev primaries	45
12. Contour Curves. Bohr potential and 1000ev primaries	46
13. Potential Function Curves.....	47
14. Impact Triangle, General Results	48
15. Gibson II Potential, 5000ev Primaries.....	49

1. INTRODUCTION.

The subject of crystal bombardment by energetic ions or atoms may be discussed from either external effects or internal interactions. Neither phenomenon is well understood, nor have adequate theories been devised to explain these interactions. One external effect is described by the sputtering ratio, which is defined as the ratio of ejected atoms from a crystal per impact atom. A more general term for crystal modification caused by incoming energetic atoms is radiation damage.

When incoming atoms or ions (called primaries) penetrate the crystal, a series of collisions may take place in which the primary energy is distributed to the crystal atoms. Often crystal atoms leave their sites and become moving atoms called secondaries. The orientation of the crystal, relative to the primary beam direction, is a critical parameter in any description of the interactions that take place. Deeper penetrations occur when primaries enter more open or transparent channels in crystals.

The primary energy effectively categorizes the type of interaction which will occur. Heavy incoming atoms with relatively low energies usually interact with the atoms of the crystal through elastic collisions. Such atoms deviate markedly from straight line trajectories. High energy primaries interact by ionization and electron excitation of the crystal

and, as a result, lose little energy. These atoms usually follow relatively straight line trajectories.^{1*}

This study is concerned with the ranges and spread of lower energy primaries as they dissipate energy through internal elastic interactions in the crystals. Range is defined as the depth of penetration of the primary from the surface. For purposes of this study total path distance and vector range from impact point to a specified point are not needed. Spread is defined as the radial displacement of the primary from the axis of its original impact line.

These introductory sections provide a background in the recent experimental and machine calculation studies of low kev atoms and ions in crystals. The topics of sputtering and basic radiation damage are not primary objectives of this thesis. However, several good sources of information are recommended: a basic text for introductory study, by Dienes and Vineyard,² and more advance articles by Wehner, et. al.,³ Nelson, et. al.,^{4,5} and Harrison, et. al.⁶.

Although recent experimental range studies have been performed with heavy ions bombarding single crystal targets; the nature of these experiments and the lack of knowledge concerning potential functions, make the comparison between laboratory and simulation data difficult. Until recently, the only theoretical potential functions available were

* All footnotes refer to the Bibliography

those from homonuclear atomic interaction. Thus, the computer programs have used primaries and crystals of the same type, while in laboratory experiments the primaries and crystals have been different substances.

Virtual leaders in the field of experimental range studies are J. A. Davies and his co-workers at Chalk River, Ontario. Their technique is both sensitive and reliable, but requires that radioactive gas ions be used as primaries. The approach entails:

...bombarding an optically flat aluminum target with a monoenergetic beam of radioactive ions, and then measuring the depth of penetration of the incident beam by dissolving successive uniform layers of aluminum from the target surface and measuring the amount of radioactivity in each layer. The ion bombardments were carried out using an electrostatic accelerator specially designed for the purpose. The technique... (dissolving extremely thin layers of known thickness)... consists essentially of two steps: electrochemical oxidation at constant voltage in aqueous ammonium citrate, followed by chemical removal of the anodic oxide film in a phosphoric acid chromium trioxide solution. Due to the highly protective nature of the anodic oxide film, this process permits highly reproducible surface layers of metal as thin as 37\AA to be removed. ... The process may be repeated as often as desired, so that it is possible to obtain the complete range-distribution curve from a single bombardment.⁷

Some of the earlier polycrystalline range studies performed by Davies, et. al. included .7 to 60 keV Na^{24} ions in aluminum,⁷ and 2 to 600 keV Kr^{85} ions in aluminum and tungsten.⁸ All of the range distribution curves exhibited "tails" of deep penetration. This phenomenon was attributed to channeling of ions in preferred directions in the crystal. Davies, et. al.

stated,

The magnitude... (of crystal lattice effects)... particularly emphasizes the need for using either single crystals or amorphous materials in future range experiments.⁸

In a more recent study the same group⁹ studied single crystals of tungsten using 1 to 20 kev Xe¹²⁵ ions. Tungsten has a body centered cubic (b.c.c.) structure in contrast to aluminum and Cu which have face centered cubic (f.c.c.) crystals. General results of the single crystal studies were:

... crystallographic effects are even larger than those found previously in Al; furthermore the results are in qualitative agreement with the theoretical prediction for b.c.c. lattice, i.e. the (100) and (111) are the most favoured directions for channeling and the (110) and (112) are less favoured. This contrasts with the f.c.c. structure, where both theory and experiment find (110) the most favoured and (111) one of the less favoured.⁹

Lutz and Sizmann¹⁰ bombarded copper (f.c.c) single crystals with Kr ions of 10 to 140 kev. energy. Their results agreed in general with Davies' single crystal data, since they showed that 110 channel shots had deepest penetration. Further, the range distribution curves showed the characteristic tail of deep penetration (up to 4000Å⁰) for 110, 111, and 100 channels. Their 25 kev and 140 kev range distribution curves (as well as some of Davies' curves) are shown in figure 1. The experimental procedure used by Lutz, et. al.¹⁰ employed the removal of thin layers of bombarded crystal by controlled sputtering with non-radio-

active krypton ions. The radioactivity was then measured.

In conjunction with the monocrystal experiments described above and computer simulation studies to be discussed, Lehmann and Leibfried¹¹ have studied the behavior of primaries in channels analytically. Their work used copper primaries in copper, as have the majority of computer programs. Their results, oriented toward long range penetrations, in part were:

Two potentials are used: an exponentially screened Coulomb potential after Bohr, used also in the machine calculation and thought to give an adequate description for relatively high energies and small interatomic distances; and a purely exponential potential after Born-Mayer, better suited for relatively low energies and large atomic distances. The maximum ranges are very large, for 10 kev in the order of 10^3 lattice parameters for the Born-Mayer potential and up to 10^7 for the Bohr potential. Presumably, the Born-Mayer potential is a better description for these events. The investigation is confined to motions near the channel axis.

2. COMPUTER SIMULATION STUDIES

This project studies the interactions of energetic atoms in crystals through the use of a digital computer simulation program. This section will present a general orientation of the use of computer simulation programs and will discuss the current work in this area. (A more detailed discussion of the program and model used in this study will be presented in section four and in Appendix II.)

Simulation programs for any system have the following three essential ingredients. (1) The system or phenomenon has a status. This status is described in terms of attributes. In the case of a crystal, such attributes as position, velocity, mass and energy are essential. (2) The status is changed or modified by an event. Events cause the atoms to leave their sites, gain or lose energy, etc. (3) The third essential element of a simulation program is time. The status and events are strongly intertwined in a time continuum. The control of the occurrence of events is critical.

Three basic approaches to simulation programs of atom-crystal interactions that have been used to date are: (1) random target atoms (i.e. lattice effects are neglected), (2) binary collision in a lattice, and (3) many body collision in a lattice. The binary collision assumes interaction with one atom at a time, while the many body approach (called n-body) simultaneously accounts for forces from several crystal atoms.

One of the earliest computer studies was made by Gibson, et. al.¹²

Their model placed the copper atoms on sites in the f.c.c. crystal and used an n-body approach. To simulate an infinite crystal, additional forces were added to the surface atoms. Because the potential functions and their corresponding force functions were not known precisely, Gibson, et.al. used "a simple central difference procedure...which gives reasonable accuracy."¹² Their techniques used $f=ma$ in an iteration procedure. This study showed evidence of chains in the 100 and 110 directions. A chain is defined as the propagation of energy along close packed rows of atoms in a crystal without mass transport. Interatomic potential, surface effects, lattice defects, and other low energy (<400 ev) phenomena were studied.

The random lattice mentioned above was used in an earlier study by Oen, et. al.¹ for copper primaries in solid copper. Their program assumed independent binary collision (accomplished by an impact parameter restriction of one half the nearest neighbor's distance), classical scattering, and the Bohr hard sphere approximation to the Bohr potential. They concluded:

It is found that neither the hard sphere approximation nor the inverse r squared approximation to the Bohr potential is particularly good. To obtain correspondence with experimental results it is found that the Bohr screening length must be increased as the atomic number of the interacting atoms increases.¹

A more recent program by Robinson and Oen¹³ (hereafter referred to as RO) used the binary approach again, but replaced the random distribution with a copper f.c.c. lattice. This program studied several potentials: the Bohr, eroded Born-Mayer, and truncated Born-Mayer. The Born-Mayer potential selected by RO had the same parameters as the Gibson II potential, but incorporated four different truncation values.

Significant among their conclusions were the following:

(1) Ranges of primaries were strongly dependent on direction, and in f.c.c. crystals the order of range was $(011) > (001) > (111) \approx$ isotropic.

(2) Larger range values were due to many glancing collisions that confined the primaries to regions of low potential. This phenomenon of deep penetration is called channeling.

(3) The combination of Bohr potential and 1000 ev primaries impacting in the (011) direction produced several primaries that moved from channel to channel. That is, RO found that the primaries showed large spread as they penetrated the crystal. Such spread was attributed to the nature of the Bohr potential, (see figure 2, which is a projection of their (011) channel trajectories onto the (011) plane. Note that three of the four tracks show large amounts of spread.)

A more recent n-body model was used by Gay and Harrison¹⁴ (hereafter referred to as GH). They used an iteration procedure, but one that has important differences from Gibson's approach (see Section 4). Further, the crystal size was smaller than Gibson's, and the program was simplified to reduce computer time. A comparison between binary collision characteristics and n-body collision approximations was performed. In general terms, the report showed that binary collision approximations approach true n-body collisions for small impact parameters. But at larger impact parameters the binary collisions have less energy transfer from primary to target, reduce the primary scattering angle and slightly increase the recoil angle. Their work provides specific quantitative results for interactions in terms of energy exchanged, scattering angles, and recoil angles.

A modified form of the GH model was used in this study.

3. STUDY OBJECTIVES

This study of energetic atoms in crystals was performed using an n-body model approach, incorporated in a computer simulation program. Specifically the study objectives were:

(1) The verification and more explicit delineation of the spread phenomenon found by RO,¹³ (figure 2). As mentioned earlier, three of the four copper primaries shown in the figure drifted considerably in the lateral direction as they penetrated the crystal.

(2) The determination of the range distribution curves for copper atoms penetrating the (011) surface of f.c.c. copper crystals. Specific attention was placed on the effect of impact point on primary range and spread.

4. SIMULATION MODEL

A. Model Discussion

The original purpose of the GH program was a comparative study of binary versus n-body collision processes. Their model used a 63 atom f.c.c. microcrystallite. These atoms were capable of movement but could not dissipate energy except by further collision. No surface effects were allowed ; which was clearly justified by the short time span of the program . An outer shell of immovable atoms was used to simulate a continuation of the lattice and test for complete event containment. (This shell is eliminated in the current program).

The objectives of the GH study were oriented toward analysis of the primary atom and one "target" atom. Concentration on the primary's history allowed a streamlining of the program that removed unneeded operations and reduced program run time. Essentially, the computation and recording of the motion of the remaining crystal atoms were deleted. This deletion was possible since the path of a primary is rarely exposed to feedback from target interactions. In analogy, if the path of radiation damage is represented by an expanding "tree of interactions", then the primary is usually spearheading the top branches.

Another result of the concentrated study on a primary and a single target was the reduction in crystal size. It must be made clear that the reduction in crystal size has been carefully studied in earlier work by Harrison.¹⁵ Considering the uncertainties of the crystal potentials and

the use of iteration techniques, the neglect of more distant crystal atoms is not significant in regard to primary performance. The crystal reduction was carried out experimentally through trial runs on the computer. The size was reduced until the program run time was optimized, but iteration results still correlated closely.

The unit crystal used in this study regenerates itself in one of two ways. The first form constructs the crystal in the y direction only (figure 3) while the second, slower program can construct the crystal in any direction (figure 4). As a result of these features, the small unit crystal is repeatedly remade in front of the primary. The fast running program is used in those cases where the primary is not expected to experience severe collisions nor deviate greatly from its original track. This type of program is called Chan2. The second program is used in areas when the primary does experience large amounts of spread and is designated Chan 3. Figures 3 and 4 indicate the unit crystal sizes and their orientation. All primaries hit the 011 surface orthogonally (i.e. in the y direction). The crystal is positioned by the program with 011 surface in the x-z plane and with the positive y direction coinciding with the primary track at impact. A majority of the runs were made in a triangular impact area. Several check runs were made in the adjacent triangle and a few elsewhere. Detailed discussion of the impact triangles is given in the next section.

The basic building block of a copper crystal is a cube measuring 3.614A on a side. The simulation program uses units of length of 1.807A called

lattice units.

The program is written in Fortran and Symbolic Fortran (an assembly language closely related to machine language). All runs were conducted on a Control Data Corporation 1604 computer which has a storage capacity of over 32,000 words and six index registers. A CDC 160 computer was used to automatically plot graphic projections of the primary trajectories. Refer to figure 5 for an example of such tracks projected onto the 011 plane.

The program constructs the lattice (i.e. assigns positions to each atom), commences the run, at designated time intervals computes the forces on the primary and secondaries, adjusts their motion accordingly, prints required information at set intervals, and "shuts down" when any of three conditions exist. The program terminates when (1) the energy of the primary goes below 25ev, (2) a preset time limit is exceeded (measured in program cycles; 10 cycles \approx time for the primary to travel one lattice unit), or (3) the primary leaves the lattice (necessary for Chan 2 programs only). The determination of this cycle factor received considerable study by Gay¹⁶ and was optimized experimentally.

As may have been evident in the brief program description above, the critical phase of the program is the method of computation of the primary path as it experiences crystal forces. In general, the "events" of this simulation program are the primary crystal interactions.

The interaction routine used by GH is still used in this model. It consists of a double iteration procedure that calculates the average force on an atom over a small distance of travel. This force is used to advance the atom.

Harrison¹⁴ states:

The unbalanced force . . . (on the primary) . . . is an average force calculated by a double iteration procedure as follows: (1) assume an atom at position 1 with velocity 1; (2) calculate the total force on the atom as a result of all the other atoms in the lattice (this means normally only about 8 - 10 nearest atoms. . .); (3) call this calculated force, force 1, and use the equation of motion to move the atom to a temporary position, position 2; (4) now repeat the force calculations for position 2, call this force 2; (5) go back to position 1, and use the average of force 1 and force 2 to move the atom to a new position, position 3. Procedures 1 through 5 constitute one "time step".¹⁴

The equation of motion used in the iteration procedure differed in two ways from the equation used by Gibson¹² et. al. Although derived in a different manner, the GH equation can be compared more easily to the Gibson form by starting with the latter and indicating the modifications.

The Gibson form of the equation (in the x direction only) is:

$$X_i(t + \Delta t) = X_i(t) + \Delta t \left[v_i(t + \Delta t/2) + m^{-1} \cdot F(t) \cdot \Delta t \right],$$

where X_i = initial X coordinate, t = time, Δt = time increment for change of position, v_i = initial velocity, m = mass, and f = the initial force.

Because Δt is a small number compared to t the term $v_i(t + \Delta t/2)$ may be expanded in a Maclaurin series. Neglecting all terms after the first, the following form is obtained: $X_i(t + \Delta t) = x_i + \Delta t \left[v_i(t) + \Delta t/2 \cdot F(2)/M \right]$

In the GH derivation, the force term is an average force where

$$\bar{F} = \frac{F_i + F_f}{2}$$

and the following expression results:
$$X_i(t + \Delta t) = X_i + \Delta t \left[V_i(t) + \frac{\Delta t}{2} \cdot \frac{F_i(t)}{m} \right]$$

Thus, the GH expression resembles the Gibson expression but utilizes a more realistic force term.

B. Potential Functions

Two factors dominate all other considerations in the simulation of primary interaction in crystals. The first is the general type of model attempted. Specifically, does the program use binary or n-body collisions? Is a crystal or a random atom arrangement used? The second factor is the selection of a potential function. Many functions have been proposed; none have been singled out as best. Until good correlation between experiment and computer simulation is made, the proper potential function will remain uncertain. In a sense this report and all such simulation studies are an attempt to locate the correct function for a particular substance.

Two basic types of potential function were used in this study: Born-Mayer and Bohr. The Born-Mayer function used has three parameter variations introduced by Gibson et. al.¹² and shown below:

$$\phi = A \exp \left[- \rho (r - r_0) / r_0 \right],$$

where r = distance in lattice units,

r_0 = nearest neighbors distance (2.555Å for copper),

l_0 = lattice unit (1.804Å for copper),

ρ = input parameter, and

A = input parameter (ev).

The form shown above is convenient for computer calculation. The three sets of parameters selected by Gibson are:

Potential	A(ev)	ρ
I	.0392	16.97
II	.051	13.00
III	.1004	10.34

To speed calculation, the Born-Mayer force functions were truncated at $f=10^{-11}$ newtons (corresponds to approximately $3\overset{\circ}{\text{A}}$).

In similar format the Bohr potential function is:

$$\phi_b = \left[\frac{1}{r} \right] \exp \left(\frac{c_b}{a_b} - r/a_b \right),$$

where r = distance in lattice units,

a_b = input parameter in lattice units, and

c_b = input parameter in ev.

The two parameters are : $c_b = 9.94 \times 10^4$ ev, and $a_b = .06741u$. These parameters are the ones used in the RO report. Further, the corresponding force truncation value was used so that the Bohr potential functions and force functions in this study are identical to Robinson's. (The truncation of the force function occurs at $f = 3.9 \times 10^{-9}$ newtons).

The lattice has zero kinetic and potential energy prior to primary impact. In other words no vibrational energy is present.

C. Binary vs n-body model

This study made use of an n-body simulation program in contrast to the simplified binary collision approach of Robinson,^{1,13,17} et. al. The in-

herent danger of superimposing independent collisions is that simultaneous collisions will not be properly accounted for. For purposes of fast computer runs, the binary program has the greatest advantage, but its justification requires better experimental verification than is yet available. The n-body program is inherently more accurate because of its more thorough interaction routine. Given proper parameters, it should yield the more accurate data.

5. EXPERIMENT PROCEDURE

Computer simulation studies are experiments in the accepted sense of the word. They are trials made to confirm or disprove some suggested phenomenon, and are subject to most of the usual experimental inaccuracies. Systematic errors occur because of improper model simulation or necessary oversimplifications of the model. Random errors caused by computer malfunction should be rare. Provided the program and its input data are not modified, the computer should reproduce results perfectly. (Refer to subsection C.).

Simulation studies are sensitive to parameter variation to the extent that some computations can become meaningless if not properly controlled. For example, the combination of high energy primaries, Bohr potential, and selected impact points produce an interaction so weak that the program cannot maintain the energy check. As a result the primary could penetrate infinitely. Such extreme situations have been avoided and are not included in the data of the report, but they do point out the danger of blind faith in computer "answers".

The remainder of this section will present the experimental approach used.

A. Determination of impact area and sample size

Symmetry considerations reveal that the impact rectangle shown in figure 3 or 4 represents all possible combinations of impact possibilities. That is, the rectangle is a "unit area" that, if repeated, will completely describe the 011 surface. Further, with one exception, the rectangle can be split down

the diagonal into two triangles that have point correspondence in regard to primary interaction. Consider impacts at points A' and C' (the 90 degree angles). As indicated in figure 4, atom row AB is nearer the surface than row DC and therefore "sees" the primary sooner. Now, a primary, or "bullet", striking the crystal at A' "sees" these top plane or near atoms (row AB) at a distance of 1.28\AA . However, a bullet hitting at point C' sees the top plane atoms (row AB) at a distance of 1.807\AA . Obviously, this difference effects the first interaction and subsequently alters the bullet's path and future collisions. It will now be shown that this difference in the two triangles, will cause a mild perturbation in range and spread data, and is not considered serious for purposes of this study. (The triangular impact area is desirable since it reduces the sample size necessary by one half).

A graphical correlation analysis of two critical parameters (range and spread) was performed to insure the validity of the impact triangle. In each triangle 14 points were chosen and the range and maximum spread values recorded. All points were obtained using 1000ev primaries and a Gibson II potential. Since this combination has a strong primary-crystal interaction, discrepancies between the two triangles should be maximum (figure 7). In general, good correlation was revealed. Note that the range correlation values show less correlation for deeper penetrations. This is expected since those primaries that impact further from the "corner atoms" have smaller energy loss rates and more chance to deviate. The spread terms have less correlation at small values. However, these terms are

sufficiently small so that .2 or .3 lattice unit variation between triangles does not effect the spread contour diagrams (to be discussed later). As a result of these considerations, triangle ABD was selected as the primary impact area. The error introduced by this assumption is small and is not known precisely. In future studies one area of further investigation should undoubtedly be a more thorough check of the rectangular impact area and its effect on results.

From the grid shown in figure 8, 14 impact points were selected and are labeled one through 14. For some of the runs these original 14 points were supplemented by 12 more. These points are labeled in the figure as 1A through 12A. The supplemental 12 point array was chosen to verify the selection of the basic 14 point sample size. Both the Gibson II-1000 and 5000ev studies were initially made on 14 point grids and later supplemented by 12 more data points. The range contour surfaces remained regular when the new points were added, and showed no anomalies (figure 9). Further, the range distribution curves for the 14 point and 26 point grids correlated very closely (figure 6), and established the soundness of 14 point grids. These range curves were constructed on an area rather than a point basis. That is, cross sectional areas of the contour surfaces (figures 9 through 12) were measured at specified depths of penetration. The ratio of this area to the total triangle area gives the percent of primaries stopped. In figure 9 the shaded area represents those primaries stopped within 100 lattice units. The ratio of this area to the total area provides the percent stopped at 100

lattice units. (The range curves were constructed from larger contour diagrams than those shown). The area method yields more accurate penetration curves than would a point system. Overall justification of a 14 point sample is simply the general regularity of the results.

B. Impact points A,B,C and D.

In addition to the 26 point grid, four other points were chosen on the triangle. These points coincide with the impact points in figure 3 of the RO study (three of the four points showed spread). These points are shown in figure 8 of this report and are labeled as A,B,C and D.

As an initial step in this study, the parameters of the RO "A,B,C and D shots" were duplicated as closely as possible. Later, several other combinations of bullet energy and potential were used. Table 1 shows the number of grid points investigated under each combination of parameters. As will be shown in the next subsection, many of these points were rechecked with additional runs.

TABLE 1

Impact Points Studied By Parameters							
Potential	RO ¹³ Points A, B, C, D		14 Point Grid		12 Point Grid		Symmetrical Triangle
	Energy 1000	Energy 5000	Energy 1000	Energy 5000	Energy 1000	Energy 5000	Energy 1000
Bohr	4	Point C	14	13	8	6	-
Gib II	4	Point C	14	14	12	12	14
Gib III	4	-	14	-	-	-	-

C. Reproduceability of runs.

As stated earlier reproduceability problems should not occur in computer studies. Unfortunately, the program - computer combination used in this study does fail to reproduce periodically. As a result a large number of reruns were necessary. The sample was random, but was later checked to insure that most combinations of energy, potential and run length were represented. The sample size was approximately 15 percent. It was found that the probability that a run would be reproduced exactly was 85 percent. Further, once a run was confirmed by a rerun, the probability of its correctness could be assumed to be one. The lack of perfect reproduceability has not been determined. However, it was found that those runs that deviated seemed to get out of phase, but did not vary greatly in amplitude or distance traveled. Generally, the variation of amplitude (i.e. spread) and depth of penetration were less than a few per-

cent. In one case the depth of penetration varied by about 50 percent, but the depth of penetration in this case was very short ($<8L_u$).

D. Program output.

The output will be briefly discussed here, so that subsequent discussions of data will have more meaning. The program as used in this study was designed specifically to examine only the primaries' performance. Output is made every ten cycles. Ten cycles is the time necessary for the bullet to travel approximately one lattice unit (1.807\AA). Each output yields the following data about the primary:

(1) $x, y,$ and z distances (measured in z lattice units) from the impact point (a " z lattice unit" is 1.414 times greater than either the x or y lattice units),

(2) $\dot{x}, \dot{y},$ and \dot{z} velocity values in " z lattice units" per second,

(3) kinetic energy, potential energy, and total energy in electron volts, and

(4) real elapsed time in seconds.

Except for a few 6000 cycle runs all of the simulations used a 2000 cycle cut off.

6. RESULTS AND CONCLUSIONS

The data collected from the printout sheets discussed in section five were condensed and tabulated as follows: (1) primary final energy (either approximately 25ev or the energy at the 2000 or 6000 cycle cut off), (2) depth of penetration in lattice units, and (3) the maximum spread. Recall that spread is the perpendicular radial distance (in lattice units) that a primary deviates from its initial straight line trajectory.

The type of tracks reported by RO (those of large penetration and spread) suggest the need for a word descriptive of their nature. Therefore, in this report, the term wander will apply to all primaries that exceed two lattice units of spread, but whose energy loss rate does not exceed $25\text{ev}/\text{\AA}$.

Four combinations of potential and energy were studied: Bohr and 1000ev primaries, Bohr and 5000ev primaries, Gibson II and 1000ev primaries, and Gibson II and 5000ev primaries. Since the data was collected from the impact point grids, it is best displayed using a pictorial representation of the grid. The penetration values are shown at their respective grid impact points and can be visualized as a penetration contour surface (figures 9 through 12). The pertinent data from the spread contours was summarized and is discussed below.

A. Spread results

The spread values for each impact triangle are a function of primary

energy, potential and impact point. Separate spread contours are included in the report, and are located on the same page as their corresponding penetration contours.

The results of the spread data collected are summarized below:

(1) Wander, as observed in the Bohr 1000ev primary case by RO, was found to exist for several other combinations of primary energy and potential function.

TABLE 2

Percent of primaries that exceeded 2LU spread and Percent of primaries that <u>wandered</u>				
	POTENTIAL			
	Gib II		Bohr	
	Energy		Energy	
	1000ev	5000ev	1000ev	5000ev
Percent >2LU Spread	27	54	43	25
Percent <u>Wander</u>	0	11.5	5	15

The result of RO can be generalized: When parameters are such that penetrations vary from deep to short values over the surface of impact triangle, then some of the primaries will wander. Note that the Gibson II - 1000ev series of runs does not satisfy this criteria (refer to table 2), since all the primaries had short penetrations.

From another viewpoint, if the strength of interaction between primary

and crystal varies over the impact grid from hard to soft collision, then some primaries will wander. Thus, the presence of wander is not simply a result of the Bohr potential, but is a function of the strength of interaction.

(2) A study of the spread data (figure 9 through 12) reveals that the primaries that wander are located in a particular region of the impact triangle. Note that the primaries impacting in zone A, figure 14, have large spread values while those in zone C have large penetrations. It is not surprising that the primaries that wandered were located at the intersection of zones A and C. The overlap of the two zones varies somewhat with the parameters of the run and cannot be firmly located. However, the important result is that wander is a function of impact position and is simply the transition region from the short range penetration zone to the deep penetration impact zone.

(3) The outlined rectangular area in zone C (figure 14) has primaries that have low spread. Any atom impacting this area will have large penetration and will not exceed .8Lu spread. The primaries in the remaining area of the impact triangle have at least 1Lu of spread except for a small area near point 11; the midpoint between the atom crystals. This midpoint is a symmetrical force region for the primaries and little deflection or spread takes place. Further, in the Bohr potential cases, the force curve is near cut off so that the forces on the primary are negligible. Two

regions of large spread occur between the .3 and .5Lu radii of the corner atoms. These are the zones where the primaries wander.

(4) Primaries 2, 5A, and 8A in figure 15 wandered. As shown by the "history curves" of the runs, the rate at which energy is lost is usually uniform until approximately 1000-1200ev and then the energy loss is more rapid. The general appearance of the family of curves is uniform, and one of gradual transition from short to long penetration as the impact points move from the corner atoms of the triangle to the channel area near the right angle. The short penetration curves display less regularity.

The gap in the region of 180A to 300A penetration is not an anomaly. If primaries were concentrated in the region of rapid penetration change (i.e. the "hills" of the penetration contour) then this gap would be filled. Though the crystal effect on range and spread seems logical, the rigid consistency and smooth transition is surprising. For example, if more impact points are studied, the occurrence of occasional penetrations in the range of 300A to 600A that do not wander can be expected.

In brief summary, primaries do wander if the impact point is located in a transition region from hard interaction to soft interaction. The "wander phenomenon" is part of a smooth change from one type of interaction to another.

(5) The four impact points of the RO study that wandered were investigated (figure 2). Their parameters were duplicated (Bohr truncated poten-

tial, 1000ev) to insure a valid comparison. In addition, the Gibson II and Gibson III potentials were used. The selection of the exact parameters in the Bohr case provided a comparison between the RO binary model and the n-body model.

Of the four points, only point C displayed wander and it did so with the following combinations of parameters: (1) Bohr and 1000ev primaries, (2) Bohr and 5000ev primaries, and (3) Gibson and 5000ev primaries. As seen in figure 14, points A, B, and D are in zone C and are typical of that zone since they displayed deep penetration and less than .8Lu spread. The probable reason for the disagreement between the RO study and this study is the use of the n-body model. (Refer to the next subsection for detailed comparison of the results obtained from the two models.)

At present, none of these results can be verified experimentally. If the potential functions studied are not reasonable, the conclusions discussed above could be radically change. As will be seen in the next section, the potential functions selected (particularly the Bohr) may be too weak. If so, the amount of "wander" found in future studies using "harder" potentials may decrease or disappear.

B. Penetration results

The penetration results are shown in contour diagrams (figure 9 through 12) and the integral penetration curves of figure 6. Penetration contours for all runs are regular and well defined. The following points are reveal-

ed from the data:

(1) Impact points 4, 4A, 7 and 7A, which are located in the 110 channel of the crystal have maximum penetration. The Gibson II-1000ev contour is complete and reveals the smallest and lowest peak of maximum penetration. The Gibson II-5000ev contour is virtually complete (four runs truncated at 600Lu) and is shaped similarly to the Gibson II 1000ev contours. However, the contour height is much greater and the region of very low penetration (below 20Lu) is much smaller.

Both Bohr contours were truncated at 2000 cycles. In comparison to the Gibson results, the areas of low penetration are smaller and the rate of change to deeper penetration more rapid. Excessive computer run time curtailed the construction of complete contour surfaces for the Bohr potentials.

The Bohr-1000ev contour and the Gibson II-5000ev contour are similar in size and shape, which indicates that these combinations of energy and potential produce similar interactions.

(2) As the energy of the primary is increased the depth of penetration increases; also, the amount of penetration varies with the potential function used.

The n-body integral penetration curve (5000ev and Gibson II potential has much larger penetrations than the RO results (figure 6). Un-

fortunately, none of these simulation curves can be easily compared to the experimental data of figure 1, because of the large difference in the substances studied. Important conclusions are available from the results, however.

The 5000ev curves in figure 6 of RO and this study agree fairly close in the region of small penetration (up to 120\AA). Thus, it is probable that the n-body program agrees closely with the binary model for severe interactions (i.e. small impact parameters below $.3L_u$ or $.5\text{\AA}$). A thorough study by GH established the close agreement between single binary collisions and n-body collisions at short impact parameters. Their study investigated a wide range of energies and several potentials (including the Gibson II).

(3) In the region of deep penetration the two models disagree. Nevertheless, an important fact was revealed when the simulation penetration data were compared with the corresponding potential curves. Refer to figure 13 which shows the Gibson II potential discussed here, the Bohr potential, and a new potential to be explained in the next subsection. As seen in the diagram, the three curves in question use the basic Gibson II potential function. However, RO curves B and C are truncated at much larger potential values than the potential of this study. As seen from the integral penetration curve and these potentials, as the distance to the truncation point is increased, the depth of penetra-

tion of the primaries increase . (This effect is opposite of what might be first supposed). The most plausible explanation probably lies in the subtle effect of the small potential curve slope (hence small force values) that occurred in the region beyond the truncation of the RO curves. These small forces confine the primaries to the more open crystal regions. As an analogy, the deeper penetrations can be compared to a rock skipping over the surface of water. It makes many weak impacts that confine its movement. This is the case of the n-body potential. The more radically truncated potentials of the RO study probably cause abrupt interaction when a primary moves from a region of no potential to one of large finite value. Thus, deep penetration of primaries still occurs in the RO model but to a much smaller extent.

In summary, one significant factor causing the deeper primary penetrations of this study was the use of a potential that was truncated at large radii. The use of the n-body model also contributed to large penetrations and will be discussed shortly.

(4) As shown in figure 13, the RO study also used an eroded potential that decreased to zero at $1.27A$. The corresponding integral penetration curve is similar in appearance to the n-body penetration curve of this study, but has slightly lower penetration values. Thus, the potential function if eroded or truncated at large distances tends to produce similar large penetration depths. In contrast, potentials that have signifi-

cant values at truncation reduce penetration depth.

(5) Another factor, which undoubtedly caused the deeper penetrations found in this study, is the n-body model. It's use insures a continual superposition of all significant crystal forces; and consequently, the net force on the primary is usually smaller and produces less scatter. Thus, the wander detected by RO for impact primaries A,B, and D, but which was not verified using the n-body model, may result from the insufficient superposition of forces in the binary approximation collision process. This helps clarify the results in the previous subsection concerning wander.

C. Recommendations

Two proposed simulation studies are presented in this subsection. Both are attempts to obtain verification with experimental data. Recent studies by Abrahamson¹⁸ provide potential functions for tungsten and the inert gases. This development, in conjunction with the experimental work of Davies, provides, for the first time, the possibility of positive experimental verification of computer simulation programs.

It is recommended that the n-body program incorporate the new potential function developed by Abrahamson, and that it be used to simulate the Davies experiment of Xe¹³⁵ in tungsten.

Although the experimental results for copper primaries in copper are not available, it is felt that the simulation penetration values are too

large (especially the n-body) and should agree more closely with the 25 keV - Kr⁸⁴ in Cu experiments and the Xe¹³⁵ in Cu experiments at 5keV. In this regard RO have used "Cu" primaries of triple mass (Cu¹⁹²) which did reduce penetration ranges (fig. 6), but not sufficiently to agree with the results of 25keV Kr⁸⁴ in Cu.

In spite of the probability that the n-body integral penetration curve, obtained in this study, is further from experimental fact than the RO curve, the n-body model is an inherently more accurate approach. This conclusion is based on previous discussion which reduces to the essential fact that the n-body model is more realistic and, hence, a better simulator. Equally critical, the results of the RO study were obtained using severe truncation values (fig 13). Truncation of the force function at significant values is unrealistic and probably leads to incorrect results. To obtain closer verification of experimental results, stronger potential functions may be necessary in future n-body program studies. (It is possible that experimental integral penetration curves could be verified by most models by sufficient adjustment of the potential functions. Thus, experimental verification in a single area will probably not prove sufficient, in the long run, to establish a particular potential function).

Preliminary calculations indicate that the potential function of Abrahamson (Xe in W) is significantly stronger than the Gibson II poten-

tial. If so, it is likely that this potential will produce excessive
duction in primary penetrations and its use in a simulation program will
not yield close correlation to Davies experimental work.

It is also recommended that the verification of Davies experiment
be attempted using a "compound" force function. This function should
follow the Gibson II force curve at small impact parameters where
good agreement is obtained at present. At approximately 1.0A the
curve would change to a different exponential form that exerts much
larger long range forces on the primaries. This function will reduce
deep penetrations and agree more closely with experimental data. The
parameters of Davies Xe in W should be duplicated for this study also.

Key
 — Xe¹³³ in W (Davies et. al.⁹)
 --- Kr⁸⁵ in Cu (Lutz et. al.¹⁰)

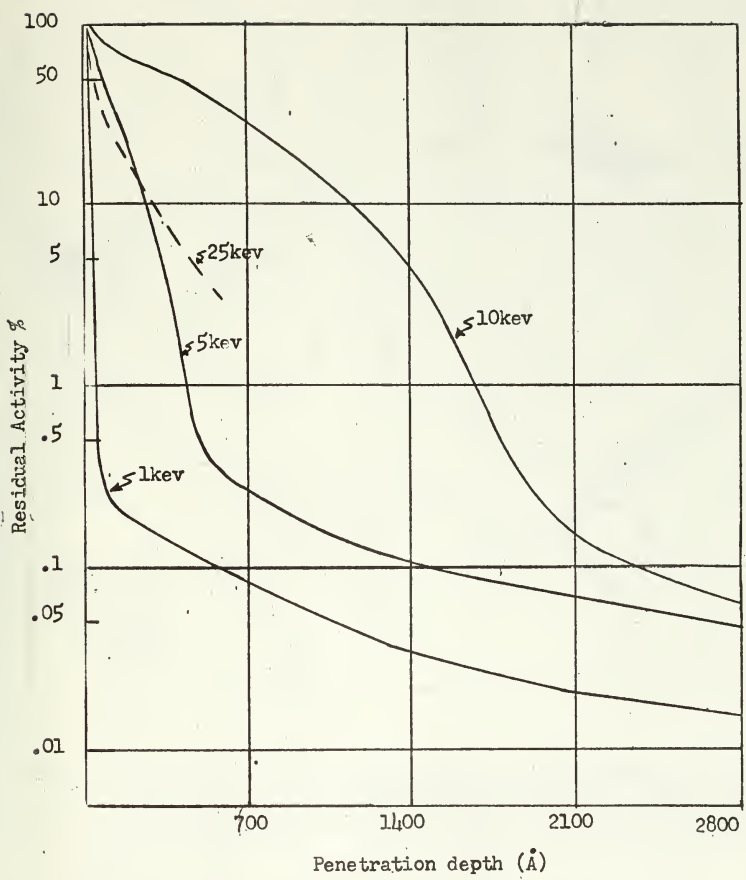


Fig. 1. INTEGRAL PENETRATION CURVES

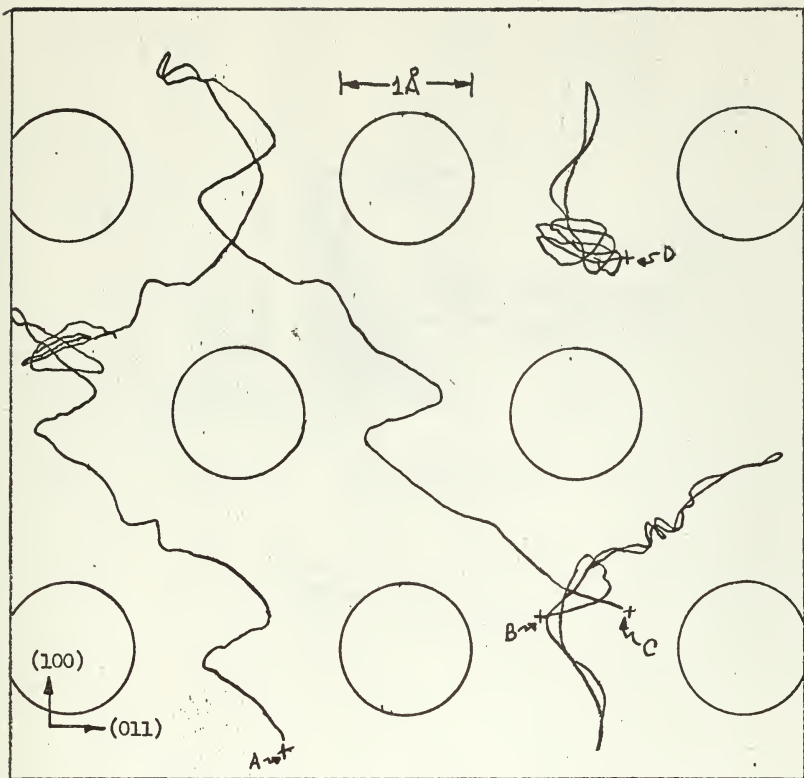


Fig. 2. ROBINSON AND OEN "... (011) channel trajectories onto $(01\bar{1})$ surface for f.c.c. Cu... (1Kev Cu primaries)... Bohr potential." 13
 Points A, B, C and D penetrated 300 \AA in part of trajectory shown.

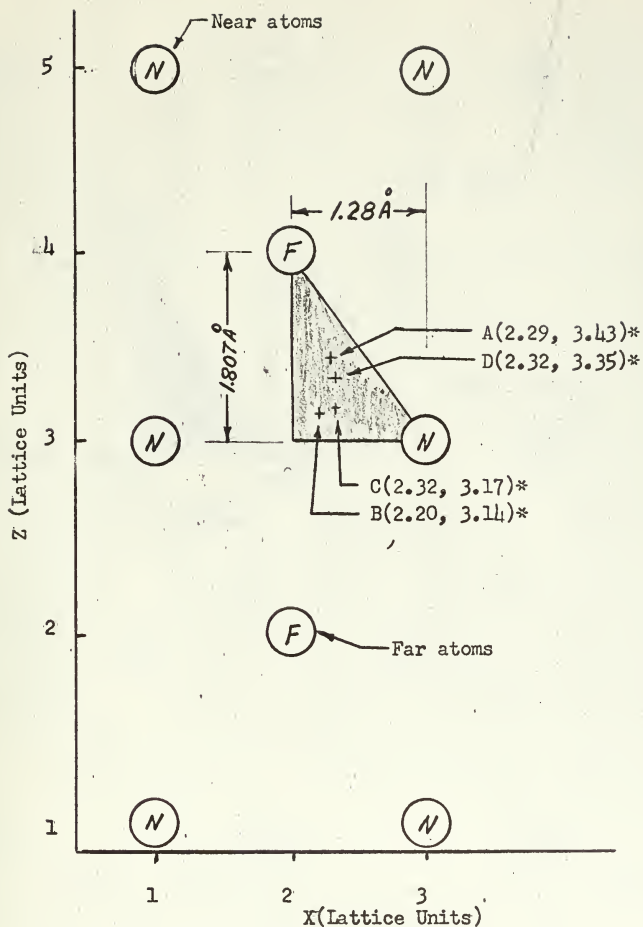


Fig. 3. (110) FACE OF CHAN₂-TYPE CRYSTAL. Shaded triangle indicates impact area; (*) RO⁻¹³ "wander" impact point coordinates.

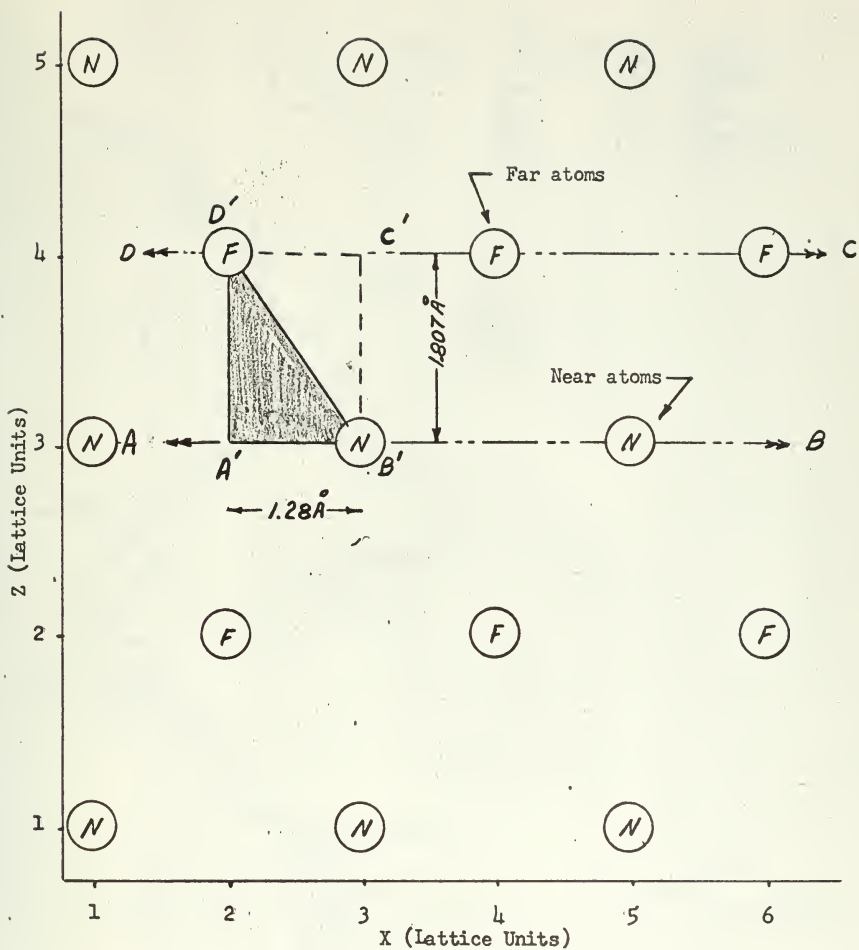


Fig. 4. (110) FACE OF CHAN₄ TYPE UNIT CRYSTAL. Shaded triangle indicates impact area.

<u>Point</u>	<u>Key</u> <u>Primary Energy</u>	<u>Potential</u> <u>Function</u>
C	1Kev	Bohr
5A	5Kev	Gibson II
4	5Kev	Gibson II
1A	1Kev	Gibson II

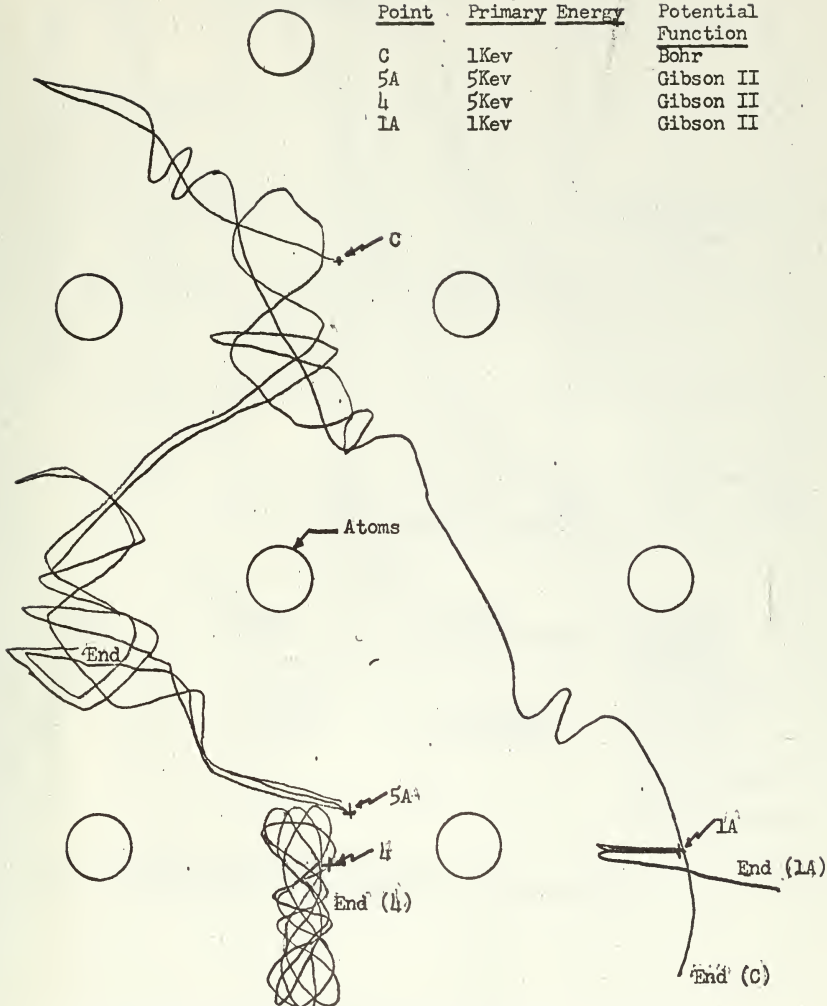
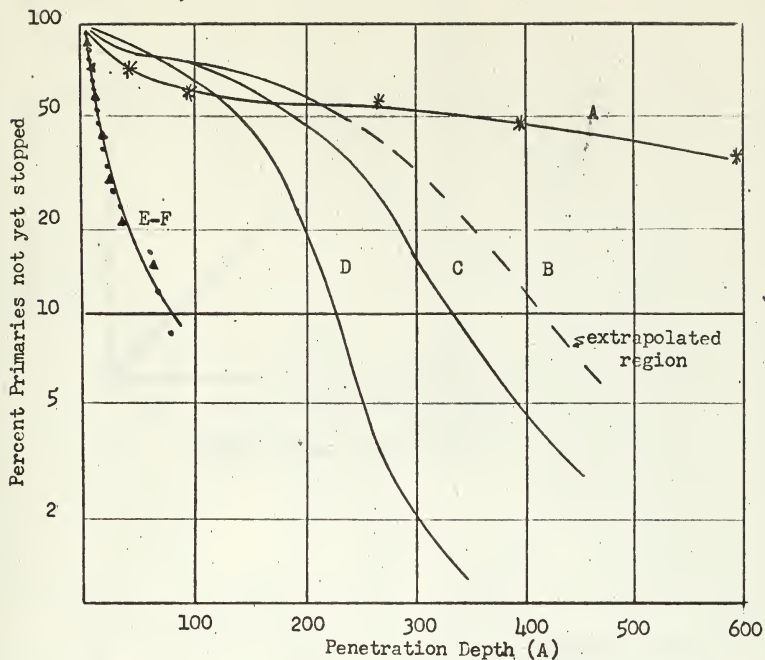


Fig. 5. N-BODY MODEL TRAJECTORIES (projected onto O11 surface).



KEY

<u>Curve</u>	<u>Model</u>	<u>Primary</u> <u>(energy in kev)</u>	<u>Potential</u> <u>Function</u>
A	N-body	5	Gibson II
B	Binary ¹³	5	Born-Mayer II
C	Binary ¹³	5 (AMU=64)	Born-Mayer I
D	Binary ¹³	5 (AMU=193)	Gibson II
E	N-body	1	Gibson II (14 pt. sample)
F	N-body	1	Gibson II (26 pt. sample)

Fig. 6. INTEGRAL PENETRATION CURVES.
(Curves E and F are essentially superimposed.)

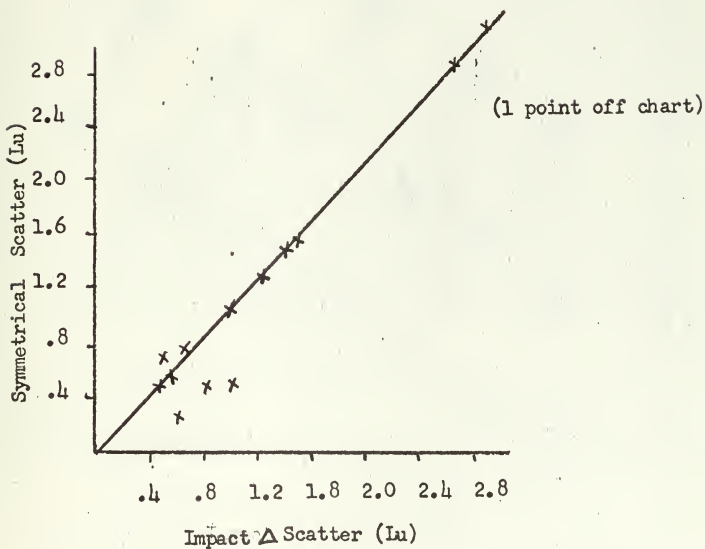
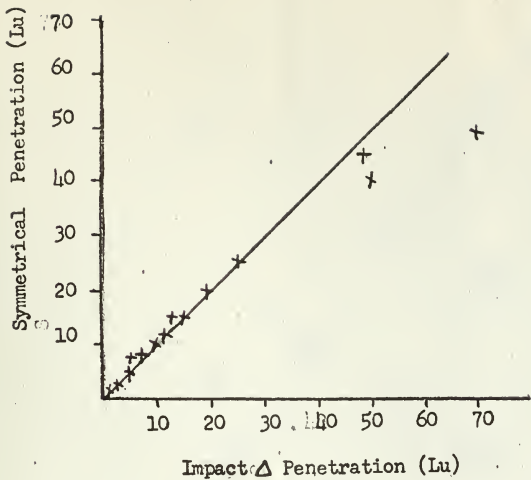


Fig. 7. DEPTH OF PENETRATION AND MAXIMUM SCATTER CORRELATION PLOTS (impact Δ vrs. symmetrical Δ).

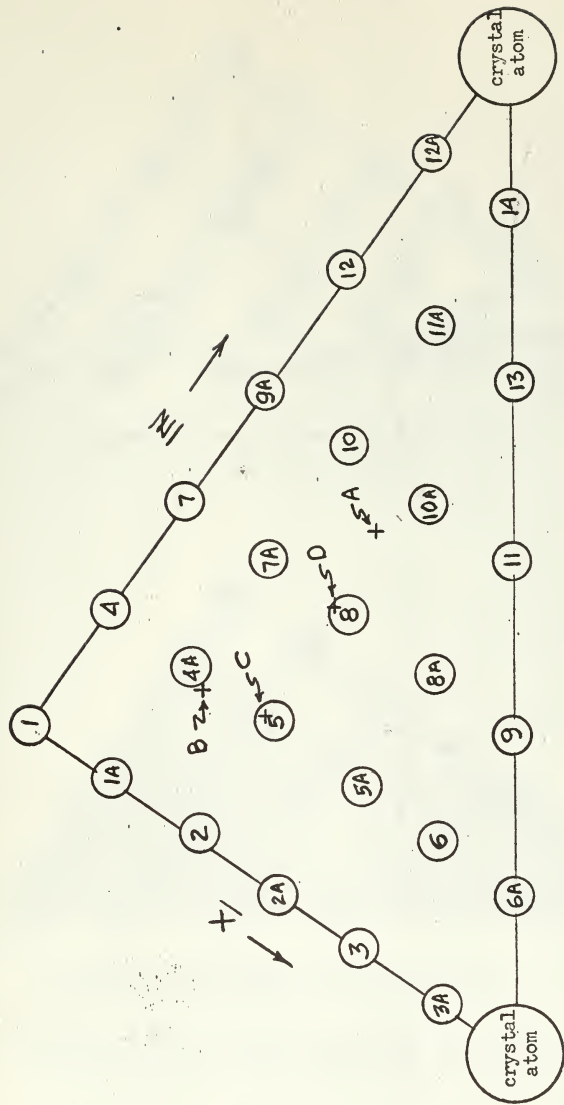
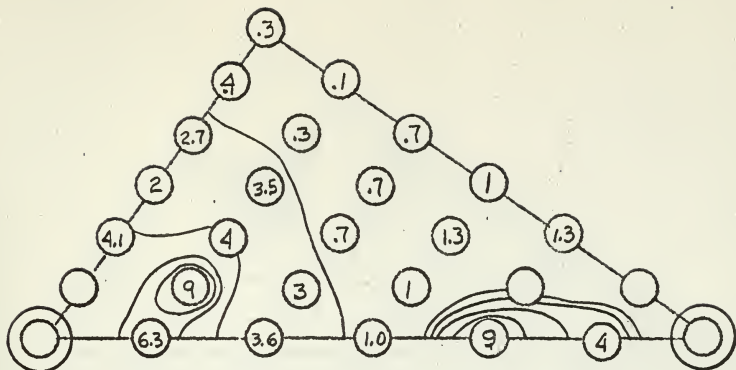
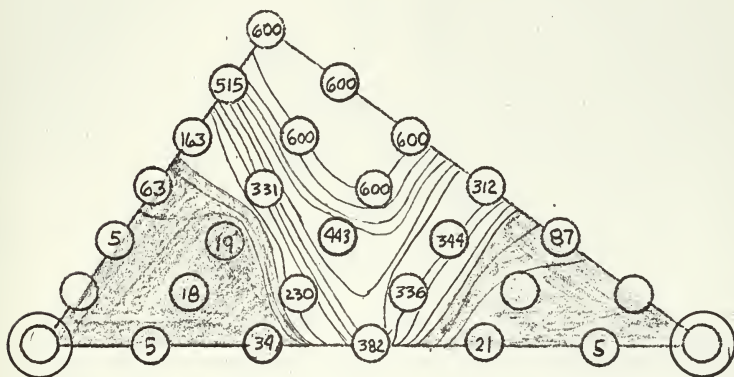


Fig. 8. IMPACT TRIANGLE. (Shows 14 and 12 point grid systems. Points A, B, C and D are RO-3 "wander" impact points.)

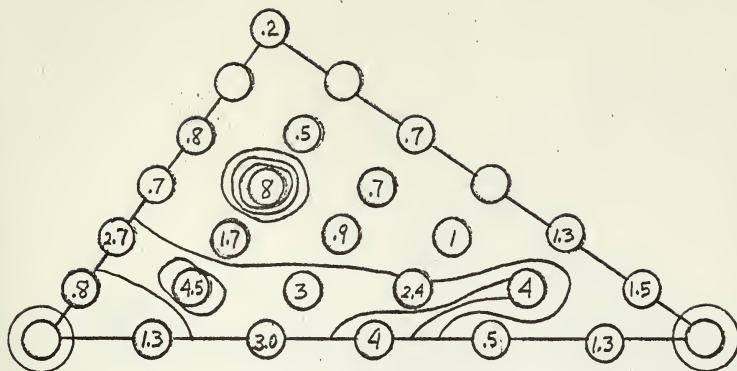


Maximum Scatter Contour (in Lattice Units)

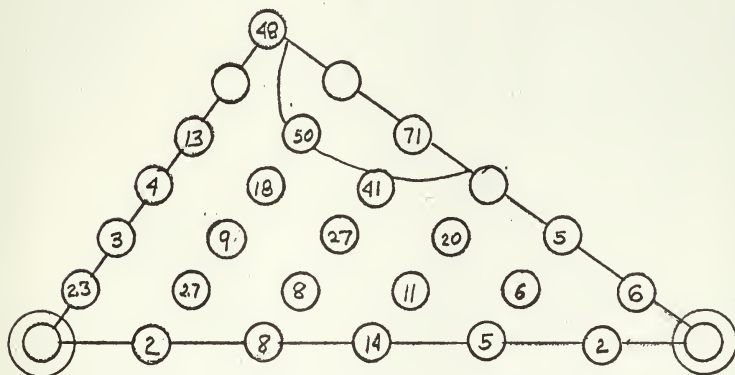


Penetration Contour (in Lattice Units)

Fig. 9. CONTOUR CURVES. Gibson II potential and 5000ev primaries.

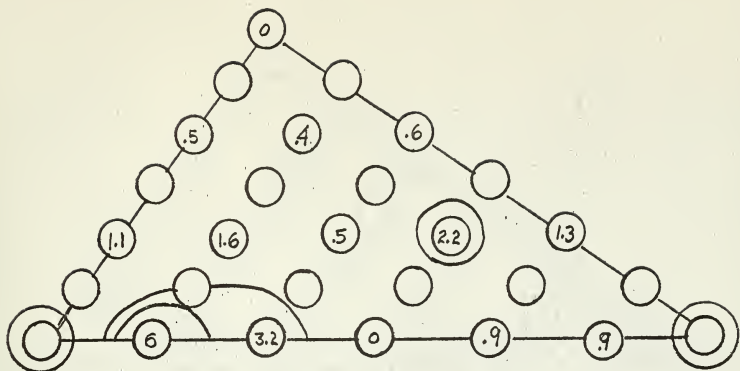


Maximum Scatter Contour (in Lattice Units)

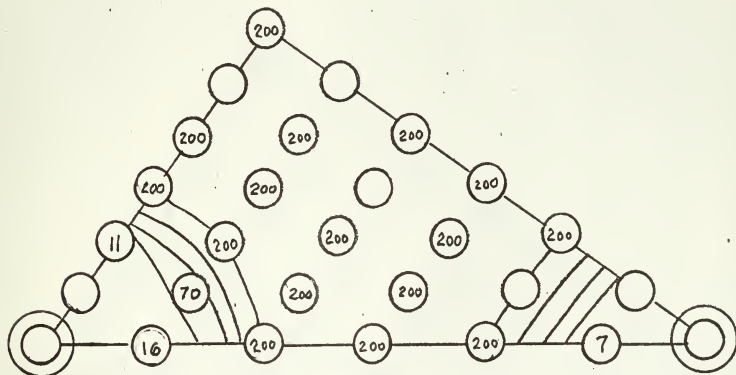


Penetration Contour (in Lattice Units)

Fig. 10. CONTOUR CURVES. Gibson II potential and 1000ev primaries.

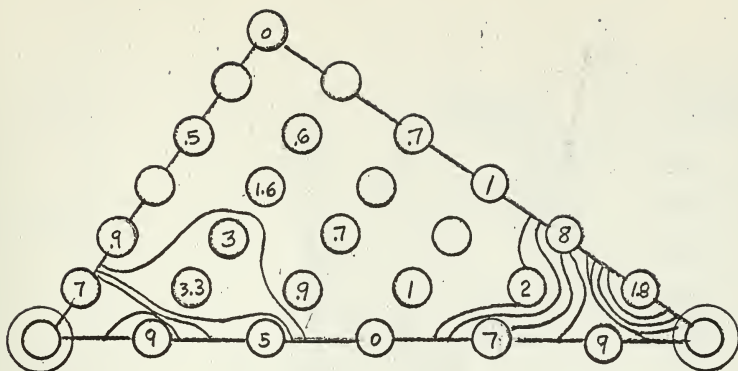


Maximum Scatter Contour (in Lattice Units)

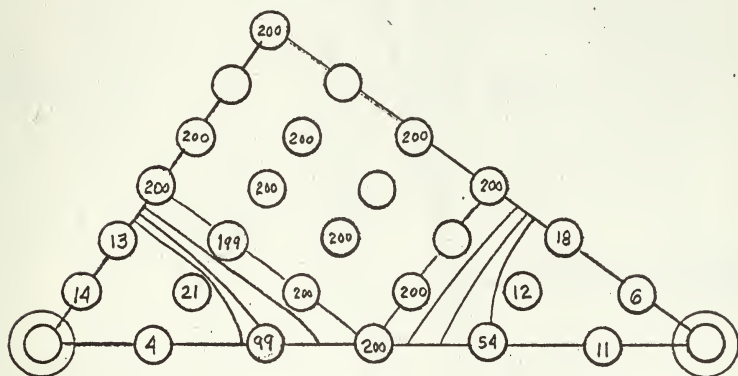


Penetration Contour (in Lattice Units)

Fig. 11. CONTOUR CURVES. Bohr potential and 5000ev primaries.



Maximum Scatter Contour (in Lattice Units)



Penetration Contour (in Lattice Units)

Fig. 12. CONTOUR CURVES. Bohr potential and 1000ev primaries.

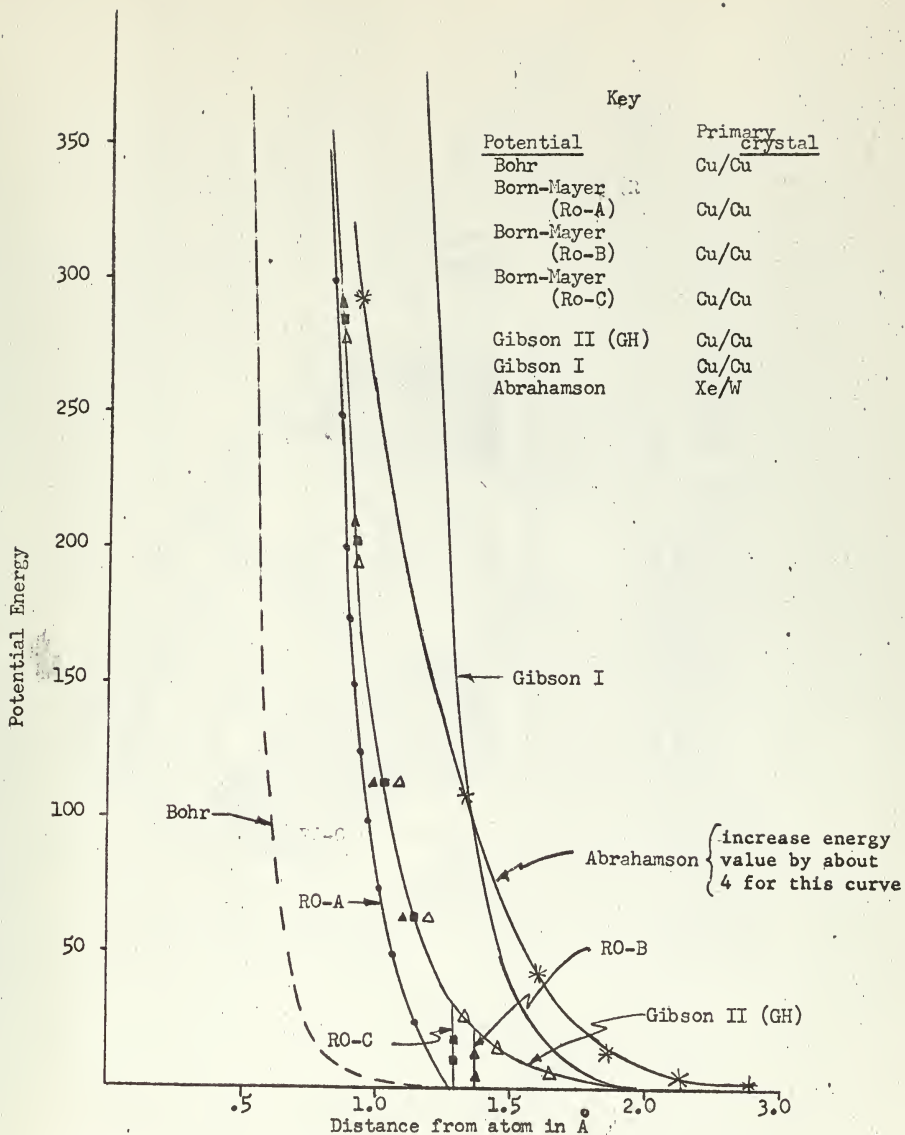


Fig. 13. POTENTIAL FUNCTION CURVES

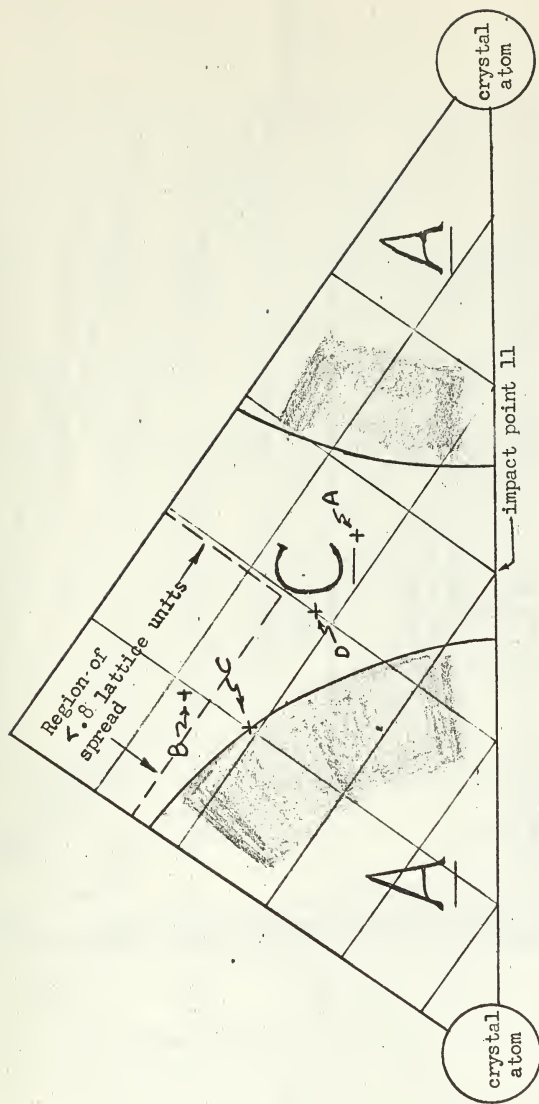


Fig. 11. IMPACT TRIANGLE. (Shows general results of study.)
 Zone A: Region of large primary spread.
 Shaded area describes region in which wander may occur.
 Zone C: Region of large primary penetration. (Zones do not apply to 1000eV Gibson II data.)

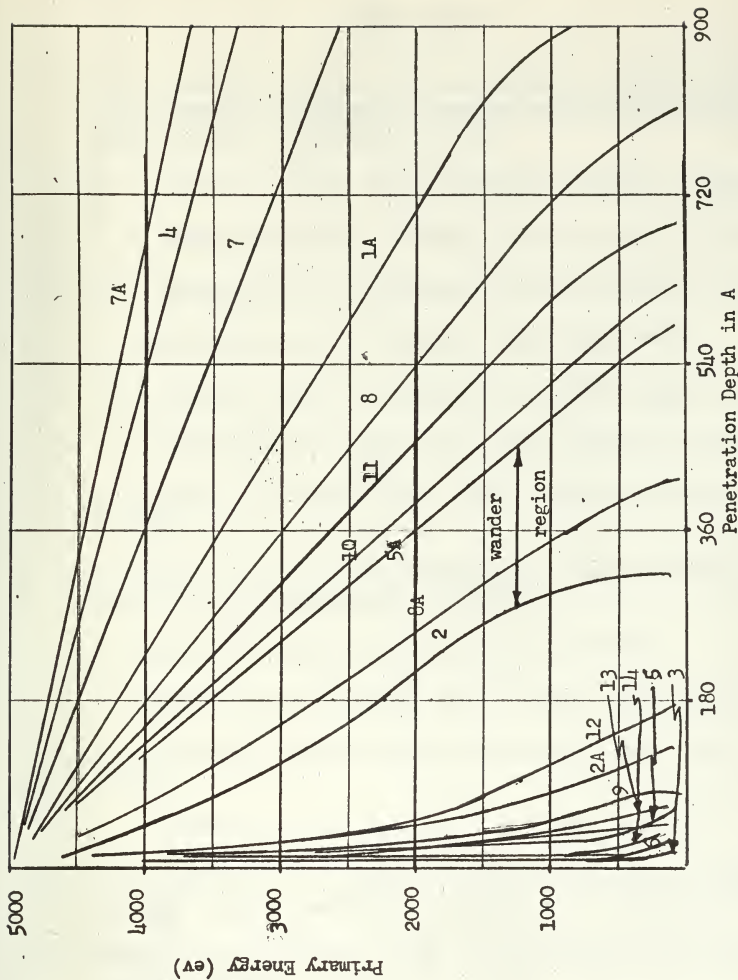


Fig. 15. GIBSON II POTENTIAL, 5000ev primaries. Indicates rate of loss of energy of primary as function of impact point.

BIBLIOGRAPHY

1. D. K. Holmes, The Ranges of Energetic Atoms in Solids, International Atomic Energy Agency Symposium on Radiation Damage in Solids and Reactor Materials, (1962).
2. G. J. Dienes and G. H. Vineyard, Radiation Effects in Solids.
3. C. E. KenKnight and G. K. Wehner, Jour. App. Phys. 35, 322 (1964).
4. R. S. Nelson and M. W. Thompson, Physics Letters 2, 124 (1961).
5. R. S. Nelson and M. W. Thompson, Phil. Mag. (1963).
6. D. E. Harrison and G. D. Magnuson, Phys. Rev. 122, 1421 (1961).
7. J. A. Davies and G. A. Sims, Can. Jour. of Chem. 39 (1961).
8. J. A. Davies, B. Domeij and J. Uhler, Arkiv For Fysik Band 24 nr 27 (1963).
9. B. Doemij, F. Brown, J. A. Davies, G. R. Piercy and E. V. Kornelsen, Phys. Rev. Letters 12, 363 (1964).
10. H. Lutz and R. Sizmann, Phys. Letters 2, 9 (1963).
11. C. Lehmann and G. Leibfried, Journ. of App. Phys. 34, 9 (1963).
12. J. B. Gibson, Dynamics of Radiation Damage, Phys. Rev. 120, 4 (1960).
13. M. T. Robinson and O. Oen, Phys. Rev. 132, 6 (1963).
14. W. L. Gay and D. E. Harrison, Machine Simulation of Collisions Between a Copper Atom and a Copper Lattice. To be published.
15. Personal correspondence. Prof. D. E. Harrison, U. S. Naval Postgraduate School.
16. W. L. Gay, Machine Calculations of Energy Transfer Phenomena in a Bombarded Lattice, Master of Science thesis, U. S. Naval Postgraduate School.

17. M. T. Robinson, D. K. Holmes, and O. S. Oen, Monte Carlo Calculations of the Ranges of Energetic Atoms in Solids presented at International Colloquium on Ion Bombardment, Bellevue (S. and O.), France, December 4-8, 1961.
18. A. A. Abrahamson, Phys. Rev. 130, 2 (1963).

BOX 1 cont.

```

ONE=1.0
TPC=2.1
EI=25.0
DIMENSION IH(5)
READ INPUT TAPE 2, 9010
READ INPUT TAPE 2, 9011, EX1, EXB, EXC, FXC, IH
EXC=LOGF(FXC)
EXB=LOGF(FXC)
EXA=EX1+EXC
FXA=EX1+FXC
READ INPUT TAPE 2, 9040, GMAS, IMAS, BX, BY, BZ, EV, DJI, COX, COY, NTI, NS, ND
READ INPUT TAPE 2, 9041, ITITLE(4), (ITITLE(I), I=6, 9), ITITLE(11)
WRITE OUTPUT TAPE 2, 9001
JJ = 0
LDA(GMAS), AJP3(9999).
ROE2 = 2.0
INDEX = 0
CVM=1.60E-19
CVM=1.672E-27
CVD=1.8075E-10
PGMAS=GMAS*CVM
PTMAS=IMAS*CVM
HGMAS=0.5*PGMAS/CVE
HTMAS=0.5*PTMAS/CVE

```

BOX 2

```

RO=1.0/RCE
SCX=RO
SCY=RO
SCZ=1.0
M = 2
IX=6
IY=5
IZ=5
IDX=((IX+1)*(IZ+1)+(IX-1)*(IZ-1))/4
IDZ=IX/2
IXP=(IX+1)/2
IYP=(IY+1)/2
IZP=(IZ+1)/2
IXI=2.0*SCX
IYI=IY/2
DVI=IYI
DVT=DVI*SCY
DZI=2.0*SCZ
TPOX=IYI*SCX
TPOZ=IZP*SCZ
OPNX=1.9*SCX
OPNZ=1.9*SCZ

```

BOX 2 cont.

```
XLL=SCX
ZLL=SCZ
JT=0
DO 60 J=1,IY
KT=0
DO 59 K=1,IZ
IT=0
DO 58 I=1,IX
ENQ(0) LDA(IT) LRS(1) QJP2(16) LDA(JT) LRS(1) QJP2(57) LDA(KT) LRS(1)
QJP2(57) SLJ(20)
16 LDA(JT) LRS(1) QJP3(57) LDA(KT) LRS(1) QJP3(57)
20 X=IT
RX(M)=X*SCX
X=JT
RY(M)=X*SCY
RZ(M)=KT
M=M+1
57 IT=IT+1
58 CONTINUE
59 KT = KT + 1
60 JT = JT + 1
CONTINUE
LL=M-1
LMM=LL-IDY
LMP=LMM+1
LMP=LL+2
DO 63 I=2,LL
VX(I) = 0.0
VY(I) = 0.0
VZ(I) = 0.0
63 CONTINUE
```

BOX 3

```
BE=EY*CVE
VOL=SQRTF(EV/HGMAS)
VX(1)=VOL*COX
VY(1)=VOL*COY
TIME=BY/VY(1)
COZ=1.0-COX*COX-COY*COY
COZ=ABSF(COZ)
COZ=SQRTF(COZ)
```

BOX 4

```

VZ(1)=VOL*COZ
RX(1)=SCX*BX+TIME*VX(1)
RZ(1)=SCZ*BZ+TIME*VZ(1)
DO 66 I=1,LL
  RX(I)=RX(I)
  RY(I)=RY(I)
  RZ(I)=RZ(I)

```

66

```

DT=DTI*CVD/VOL
DYS=0.0
DZS=0.0
TIME=0.0
NT=0
GRX(1) = RX(1)
GRZ(1) = RZ(1)

```

```

II = 2
WRITE OUTPUT TAPE 3,901C
WRITE OUTPUT TAPE 3,9016,IH,901C
WRITE OUTPUT TAPE 3,905C,GMAS,TMAS
WRITE OUTPUT TAPE 3,908C,COX,COY
WRITE OUTPUT TAPE 3,9012,RX(1),RZ(1),EV,DTI
WRITE OUTPUT TAPE 3,909C,BX,BZ,L1,LYP,IYP,I7P
WRITE OUTPUT TAPE 3,9014,EXA,EXP,FXA
WRITE OUTPUT TAPE 3,9060,TMAS,DTI,THERM

```

BOX 5

```

68 DTOD=DT/CVD
  HDTCM=0.5*DT/PTMAS
  QDTOM=0.5*HDTCM
  HDIOMB=0.5*DI/PGMAS
  QDIOMB=0.5*HDIOMB

```

BOX 6

```

70 DO 75 I=1,LL
75 LDA(ZE)STA1(FX)STA1(FY)STA1(FZ)
100 LDA(ZE)STA1(TPOT)STA1(TPKE)STA1(SPE)
100 IPI = I + LL
120 DO 200 J=IPI,LL
120 +SSK(DRX) = RX(J) - RX(I)
120 +SSK(DRY) = RY(J) - RY(I)
120 +SSK(DRZ) = RJ(J) - RJ(I)
120 +SSK(DR2) = SLJ(L*2) + SCM(MASK), +FSB(ROE), AJP2(200).
150 DIST = (DRX * DRX + DRY * DRY + DRZ * DRZ)
155 DIST = SORTF(DIST)
155 FORC(FM)AJP3(200)
155 FORC = FORC / DIST
155 FOD = FORC * FOD
155 FA = DRX * FOD
155 FB = DRY * FOD
155 FC = DRZ * FOD
160 FX(J) = FX(J) + FA
160 FY(J) = FY(J) + FB
165 FX(I) = FX(I) - FA
165 FY(I) = FY(I) - FB
165 FZ(I) = FZ(I) - FC
200 CONTINUE

```

BOX 7

```

LDA(INDEX)AJP1(260).
INDEX=1
I=1
RXK(I) = RX(I)
RYK(I) = RY(I)
RZK(I) = RZ(I)
RX(I) = (VX(I) * HDIOMB) * DTOD + RX(I)
RY(I) = (VY(I) * HDIOMB) * DTOD + RY(I)
RZ(I) = (VZ(I) * HDIOMB) * DTOD + RZ(I)
DO 250 I=2,LL
RXK(I) = RX(I)
RYK(I) = RY(I)
RZK(I) = RZ(I)
RX(I) = (VX(I) * HDIOMB) * DTOD + RX(I)
RY(I) = (VY(I) * HDIOMB) * DTOD + RY(I)
RZ(I) = (VZ(I) * HDIOMB) * DTOD + RZ(I)
CONTINUE
GO TO 100
250 GO TO 100

```

BOX 8

```

260 INDEX=0
    TIME=TIME+DT
    NT=NT+1
    I=1
    RX(I)=RX(I)+(VX(I))+FX(I)*CDTOM(B)*DTOD
    RY(I)=RY(I)+(VY(I))+FY(I)*CDTOM(B)*DTOD
    RZ(I)=RZ(I)+(VZ(I))+FZ(I)*CDTOM(B)*DTOD
    VX(I)=VX(I)+FX(I)*HDTOMB
    VY(I)=VY(I)+FY(I)*HDTOMB
    VZ(I)=VZ(I)+FZ(I)*HDTOMB
    LDA(ZE)STAI(FX)STAI(FY)STAI(FZ)
    DO 300 I=2,LL
    RX(I)=RX(I)+(VX(I))+FX(I)*CDTOM)*DTOD
    RY(I)=RY(I)+(VY(I))+FY(I)*CDTOM)*DTOD
    RZ(I)=RZ(I)+(VZ(I))+FZ(I)*CDTOM)*DTOD
    VX(I)=VX(I)+FX(I)*HDTOMB
    VY(I)=VY(I)+FY(I)*HDTOMB
    VZ(I)=VZ(I)+FZ(I)*HDTOMB
    LDA(ZE)STAI(FX)STAI(FY)STAI(FZ)
300 CONTINUE

```

BOX 9

```

LDA(RY+1)FSB(DYT)AJP2(LL+1)SLJ(LL+5)+ENA(L+3)SAU(L-1)+LDA(DYT)FSB(SC
1Y)+STAI(DYT)ENI(O)+SLJ4(800)ENI(O)
LDA(RX+1)FSB(XLL)AJP3(850)FSB(DXT)AJP2(870)
LDA(RZ+1)FSB(ZLL)AJP3(900)FSB(D/T)AJP2(920)
PKE(1)=HGMA*(VX(1)*VX(1)+VY(1)+VZ(1)+VZ(1))
I=1
LDA(I)PKE)FSB(EI)AJP2(310)
NS=NT
NT=NS-1
LDA(NS)SUB(NT)AJP(400)AJP3(400)
GO TO 70
400 CONTINUE
DO 500 I=1,LL
500 LDA(ZE)STAI(PRE)STAI(PTE)STAI(PKE)

```

BOX 10

```

IPI = I + 1
DO 600 J=IPI,LL
DRY=RY(J)-RY(I)
+SSK(DRY),SLJ(LL+2),+SCM(MASK),+FSB(ROE),AJP2(600).
DRX=RX(J)-RX(I)
+SSK(DRX),SLJ(LL+2),+SCM(MASK),+FSB(ROE),AJP2(600).
DRZ=RZ(J)-RZ(I)
+SSK(DRZ),SLJ(LL+2),+SCM(MASK),+FSB(ROE),AJP2(600).
DIST=DRX*DRX+DRY*DRY+DRZ*DRZ
FSB(ROE2),AJP2(600).
DIST = SQRT(DIST)
556 POTF(DIST)
560 STAI(PPE)
600 CONTINUE

```

BOX 11

```

I=1
PKE(1)=HGMS*(VX(1)+VY(1)*VY(1)+VZ(1)+VZ(1))
FAD(TPKE),STA(TPKE),LDA1(PKE),FAD1(PPE),STA1(PTE).
DX=RX(1)-RXI(1)+DXS
DY=RY(1)-RYI(1)+DYS
DZ=RZ(1)-RZI(1)+DZS
GRX(11)=RX(1)+DXS
GRZ(11)=RZ(1)+DZS
II=1+1
WRITE OUTPUT TAPE 3,902G,NT,DX,DY,DZ,VX(1),VY(1),VZ(1),PKE(1),PPE(
11),PTE(1),TIME
LDA1(PPE),FSB(BITY),+AJP3(L+1),SLJ(700),+RAD(JJ)
INA(-3),+AJP2(1000)-----

```

BOX 12

```

700 LDA(NT),SUB(NTI),AJP2(1000)
VOL=SORTF(PKE(1)/HGMS)
DT=DTI+CVD/VOL
NS=NS+ND
GO TO 68

```

BOX 13

```

800 SLJ(*)
DYS=DYS+DYT
DO 810 I=2,LMN
K=I+IDY
LDA3(VX)STA1(VX)LDA3(VY)STA1(VY)LDA3(VZ)STA1(VZ)
LDA3(RX)STA1(RX)LDA3(RY)FSB(DYT)STA1(RY)LDA3(RZ)STA1(RZ)
810 CONTINUE=LMP,LL
DO 820 I=1,LL
LDA(ZE)STA1(VX)STA1(VY)STA1(RY)LDA1(RZI)STA1(RZ)
LDA1(RX)STA1(RX)LDA1(RY)STA1(RY)
820 ENI(1)LDA1(RY)FSB(DYT)STA1(RY)
GO TO 800

```

BOX 14A

```

850 DO 852 I=2,LL
    LDA1(RX)STAI(RXK)LDA1(RY)STAI(RYK)LDA1(RZ)STAI(RZK)
    LDA1(VX)STAI(FX)LDA1(VY)STAI(FY)LDA1(VZ)STAI(FZ)
    CONTINUE
852 DO 860 I=2,LL(TOPNX)AJP2(855)
    LDA1(RX)STAI(RXK)LDA1(RY)STAI(RYK)LDA1(RZ)STAI(RZK)
    LDA1(VX)STAI(FX)LDA1(VY)STAI(FY)LDA1(VZ)STAI(FZ)
    GO TO 860
855 CONTINUE
    K=I-IDX
    LDA3(RXK)FAD(DXT)STAI(RX)LDA3(RYK)STAI(RY)LDA3(RZK)STAI(RZ)
    LDA3(FX)STAI(VX)LDA3(FY)STAI(VY)LDA3(FZ)STAI(VZ)
    CONTINUE
860 ENIL1)LDA1(RX)FAD(DXT)STAI(RX)
    DXS=DXS+DXT
    GO TO 305

```

BOX 14B

```

870 DO 872 I=2,LL
    LDA1(RX)STAI(RXK)LDA1(RY)STAI(RYK)LDA1(RZ)STAI(RZK)
    LDA1(VX)STAI(FX)LDA1(VY)STAI(FY)LDA1(VZ)STAI(FZ)
    CONTINUE
872 DO 880 I=2,LL(TPOX)AJP3(875)
    LDA1(RX)STAI(RXK)LDA1(RY)STAI(RYK)LDA1(RZ)STAI(RZK)
    LDA1(VX)STAI(FX)LDA1(VY)STAI(FY)LDA1(VZ)STAI(FZ)
    GO TO 880
875 CONTINUE
    K=I-IDX
    LDA3(RXK)FSB(DXT)STAI(RX)LDA3(RYK)STAI(RY)LDA3(RZK)STAI(RZ)
    LDA3(FX)STAI(VX)LDA3(FY)STAI(VY)LDA3(FZ)STAI(VZ)
    CONTINUE
880 ENIL1)LDA1(RX)FSB(DXT)STAI(RX)
    DXS=DXS+DXT
    GO TO 305

```

BOX 15B

```

900 DO 902 I=2,LL
    LDA1(RX) STA1(RXK) LDA1(RY) STA1(RYK) LDA1(RZ) STA1(RZK)
    LDA1(VX) STA1(VX) LDA1(VY) STA1(VY) LDA1(VZ) STA1(FZ)
    CONTINUE
902 DO 910 I=2,LL
    LDA1(RZI) FSB(OPNZ) AJP2(905)
    LDA1(RXI) STA1(RX) LDA1(RYI) STA1(RY) LDA1(RZI) STA1(RZ)
    LDA1(ZE) STA1(VX) STA1(VY) STA1(VZ)
    GO TO 910
905 CONTINUE
    K=I+107
    LDA1(RXK) STA1(RX) LDA3(RYK) STA1(RY) LDA3(RZK) FAD(DZT) STA1(RZ)
    LDA3(FX) STA1(VX) LDA3(FY) STA1(VY) LDA3(FZ) STA1(VZ)
910 CONTINUE
    ENI(1) LDA1(RZ) FAD(DZT) STA1(RZ)
    DZS=DZS-DZT
    GO TO 306

```

BOX 15B

```

920 DO 922 I=2,LL
    LDA1(RX) STA1(RXK) LDA1(RY) STA1(RYK) LDA1(RZ) STA1(RZK)
    LDA1(VX) STA1(VX) LDA1(VY) STA1(VY) LDA1(VZ) STA1(FZ)
    CONTINUE
922 DO 930 I=2,LL
    LDA1(RZI) FSB(TPOZ) AJP3(925)
    LDA1(RXI) STA1(RX) LDA1(RYI) STA1(RY) LDA1(RZI) STA1(RZ)
    LDA1(ZE) STA1(VX) STA1(VY) STA1(VZ)
    GO TO 930
925 CONTINUE
    K=I+107
    LDA1(RXK) STA1(RX) LDA3(RYK) STA1(RY) LDA3(RZK) FSB(DZT) STA1(RZ)
    LDA3(FX) STA1(VX) LDA3(FY) STA1(VY) LDA3(FZ) STA1(VZ)
930 CONTINUE
    ENI(1) LDA1(RZ) FSB(DZT) STA1(RZ)
    DZS=DZS+DZT
    GO TO 306

```

BOX 16

```

1000 II = II - 1
    CALL DRAW(II,GRX,GRZ,0,0,LABEL,ITITLE,EXSCALE,YSCALE,
    10,0,2,9,15,1,ERROR)
    STOP
9999 END
    END

```

APPENDIX II
PROGRAM DISCUSSION

A. Program Explanation

The descriptions given below are to be used with Appendix I (Program Listing), and are specifically applicable to programs Chan3, Bullet3, or G Chan3.

BOX 1

Listing of dimension, common, and Format statements. Provide graph plot data needed such as graph size, scale, and titles. Read force and potential function parameters. Read primary atom parameters. Evaluate miscellaneous constants.

BOX 2

Designation of nearest neighbor lattice distances. Construction of microcrystallite. Three nested "DO loops" that extend to statement 63 are used to locate and number the atoms in the crystal.

BOX 3

Initialize the velocity and the position of the primary.

BOX 4

Store initial positions of all atoms. Initialize various terms (i.e. set=0). Print variable quantities such as primary energy, direction cosines, mass, etc. which comprise the output heading.

BOX 5

Compute several constants given DT, CVD, PTMAS and PGMAS.

BOX 6

This entire box is a "DO loop" on all crystal atoms. Set all forces to 0. Check coordinate distances from primary to lattice atoms and neglect if greater than ROE. Compute the square of the "vector" distances between the primary and lattice atoms and neglect if greater than $(ROE)^2$. Compute the force that corresponds to the vector distance and compare it to FM. Neglect if less than FM. Compute forces on the primary and lattice atoms.

BOX 7

If index=1 jump to box 8. Compute temporary position of the primary and then the rest of the crystal atoms. All atoms are advanced at their initial velocity for DT seconds, while experiencing forces found in box 6.

BOX 8

(Return to box 6 and recompute the forces on all atoms. These values are added to the initial forces yielding force terms twice the average. Since index=1 on reaching box 7 a jump is made to statement 260 in box 8). The averages of the initial and temporary position forces are used to compute the final positions of the primary and lattice atoms. (See page 14 of text).

BOX 9

Perform tests to see if program output is necessary or if the program should rebuild the crystal. If the latter is true jump to the appropriate regeneration box.

BOX 10

Calculate the distance from the primary to each lattice atom; if less than ROE calculate the potential energy of the interaction and store.

BOX 11

Calculate the quantities needed in the output statement (i.e. primary position, kinetic energy, total energy, and real elapsed time). Write the output statement. Check to insure the potential energy is less than "Bitty". Terminate program if the potential energy is less than "Bitty" for three passes.

BOX 12

Check current program cycle. If at "cut off" cycle, terminate the program.

BOX 13

This section regenerates the microcrystallite in the +Y direction.

BOX 14A

Regenerate microcrystallite in the -X direction.

BOX 14B

Regenerate microcrystallite in the +X direction.

BOX 15A

Regenerate microcrystallite in the -Z direction.

BOX 15B

Regenerates microcrystallite in the +Z direction.

BOX 16

Call the graph plot subroutine (called Draw). The following parameters are necessary:

<u>Variables</u>	<u>Explanation</u>
II	Number of points to be plotted
GRX	X coordinate
GRZ	Y coordinate (simulation program Z coordinate)
C	Number of curves per graph
G	Point or curve plot
LABEL	Type <u>End</u> by the end of curve
ITITLE	Graph title
EXSCALE	Graph scale in X direction
YSCALE	Graph scale in Y direction
0	Distance of x axis from bottom of graph
0	Distance of y axis from left edge
2	Mode of x axis (automatic)
2	Mode of y axis (automatic)
9	Graph width
15	Graph height
1	Place grid on graph
ERROR	Indicates if previous plot was OK

B. Definition of Variables:

<u>Term</u>	<u>Usage</u>
Bitty	a small increment that is compared to primary potential energy (PTE). Used to terminate program when potential energy goes below increment value.
BE	primary energy (in joules)
BX, BY, BZ	primary initial coordinate (in lattice units)
COX, COY, COZ	direction cosines of primary
$CVD=1.8075 \times 10^{-10}$	converts lattice units to Å (Cu only)
$CVE=1.60 \times 10^{-19}$	converts ev to joules
$CVM=1.672 \times 10^{-27}$	converts AMU to kg.
DIST	distance between two atoms or the square of the distance (lattice units)
DT	basic time step length (seconds)
DTI	variable scale factor for DT
DTOD	DT/CVD (a "units converter")
DRX, RRY, DRZ	coordinate distance of primary to lattice atoms (in lattice units)
DXS, DYS, DZS	locates current microcrystallite with respect to original origin (lattice units)
DXT, DYT, DZT	test constants used to rebuild crystallite
EI=25.0	cut off energy (in electron volts)
EXA, EXB, EXC, EX1	input potential function parameters (see Gay ¹⁶ thesis)
EV	primary energy (in electron volts)

FA, FB, FC	x, y, and z force components between two atoms (in newtons)
FM	a small force increment used to eliminate weak force terms
FOD	force/distance (in newtons/lattice units)
FORCE	eroded force between two atoms (in newtons)
FXA, FXC	input force function parameters (see Gay thesis)
FX, FY, FZ	x, y, z coordinate force terms, respectively (in newtons)
GMAS	primary mass (in AMU)
GRX, GRZ	coordinates of primary that are used by graph plot routine (in lattice units)
IDX, IDY, IDZ	constants used in lattice reconstruction
IT, JT, KT	test points in lattice generator
IX, IY, IZ	unit lattice dimensions (in lattice units)
IXP, IYP, IZP	specify volume of microcrystallite (in lattice units)
IYT	used in crystal regeneration
HDTOM	$DT/(2*PTMAS)$
HDTOMB	$DT/(2*PGMAS)$
HGMAS	$1/2$ primary mass. units: $(ev*kg)/(m^2/sec^2)$
HTMAS	$1/2$ target mass. units: $(ev*kg)/(m^2/sec^2)$
M=2	a constant

MASK	used to calculate absolute value (removes minus signs)
ND	print statement increment (in cycles)
NS	initial print statement (in cycles)
NT	current program cycle
NTT	program cycle for final print statement ("cuts off program")
ONE=1.0	a constant
OPNX	1.9 SCX
OPNZ	1.9 SCZ
PGMAS	primary mass (in kg)
PKE	primary kinetic energy (in electron volts)
POT	potential between any two atoms (in electron volts)
PPE	primary potential energy (in electron volts)
PTE	primary total energy (in electron volts)
PTMAS	target mass (in kg)
QDTOM	$DT/(4*PTMAS)$
QDTOMB	$DT/(4*PGMAS)$
ROE	nearest neighbors separation (in lattice units)
RO	$=1/ROE$
RX, RY, RZ	atom coordinate (in lattice units)
RXI, RYI, RZI	initial atom coordinates (in lattice units)

RXK, RYK, RZK	temporary atom coordinates used in force calculation (in lattice units)
SCX, SCY, SCZ	factors to convert X,Y,Z to the same lattice unit basis; (values depend on type crystal used; i.e. BCC or f.c.c., etc.)
TIME	real elapsed time (in seconds)
TMAS	target mass in AMU
TPO=2.1	a constant
TPOX	2.1 SCX
TPOZ	2.1 SCZ
VOL	velocity of primary (meters/seconds)
VX, VY, VZ	atom velocity (in meters/seconds)
XLL, ZLL	test constants that determine if regeneration is necessary
ZE= 0.0	a constant

APPENDIX III
PROGRAM OPERATING PROCEDURES

The simulation model consists of a single basic program that has two forms:

(1) A fast running program that can reconstruct the basic lattice in the y direction only (the direction of the incoming bullet). This program is limited to cases in which the bullet does not interact strongly and hence doesn't leave the basic lattice in any direction except the y direction. This program runs in about one half the time of the other program and has three identical decks which are titled as follows: Chan, Gchan, and Bullet. For runs cut off as 2000 cycles the "Chan type" program requires about ten minutes. Those shots that strike the impact triangle near the corner atoms often terminate in very short time since the primary rapidly drops below the cutoff energy of 25ev.

(2) The slower program can contain any bullet trajectory since it reconstructs the lattice in any direction required. The testing procedure to perform this function increases the program run time. This program has two identical decks that are titled: Chan3 and Bullet3. (The various deck names serve only to expedite processing and ease administration of runs. The slower program (Chan3) was the third modification of the basic n-body program). Run times are about 20 minutes for 2000 cycle cases.

The items discussed in the remainder of this section are applicable

to all decks:

A. Parameter cards internal to the deck.

Within the program deck there are three parameter cards that are often changed; the potential function, force function, and the force truncation card. The force and potential cards are the third and fourth cards in all decks. These fortran functions are computed from a single input data card (see the next sub section). Thus the force and potential cards are paired to an input parameter card. Specifically, the Bohr potential and force cards have a single corresponding input card. The Born-Mayer force and potential cards become one of the three Gibson forms (I, II, or III) through the use of one of three corresponding input parameter cards. The third internal card is the force card (ex. $fm = 1.0E-11$) which allows the selection of any desired truncation force.

B. Input data cards.

These are the basic data cards used at the end of the deck to specify the various parameters for a run and to set up the graph plot routine. The following list describes the cards in order as they would appear for a single run:

(1) The first card prints any desired statement at the top of the print out.

(2) This is the force and potential input parameter card and it supplies the following values: EX1, EXB, EXC, FXC, IH. The first four quantities

are needed to define the function and the last (IH) prints the potential function in the printout. The above data cards are used once per run. (Chan5 uses a new input parameter system).

(3) This card provides the variable quantities that specify the primary parameters and general program information. The following items appear:

GMAS = Primary mass in AMU

TMAS = Lattice atom mass in AMU

BX = X initial coordinate for the primary

BY = Y initial coordinate for the primary

BZ = Z initial coordinate for the primary

EV = Primary energy in eV

COX = Direction cosines of primary

COY = From the 011 plane to trajectory line

NTT = Cut off cycle (ends program)

NS = First print statement (in cycles)

ND = Print increment (in cycles)

Recall that one cycle = .1 time for the primary to travel one lattice unit (1.807\AA).

The next six data cards are used to title and identify the graph output for the run.

- (4) Potential is designated (ex. GIB. for Gibson)
- (5) Energy (ex. 5000ev)
- (6) X coordinate (ex. x = 2.00)
- (7) Z coordinate (ex. z = 3.00)
- (8) Cosine X (ex. cox = .00)
- (9) Cosine Y (ex. coy = 1.00)

This completes the data cards needed for single run.

To provide additional runs cards three through nine are repeated for each run. An "end card" is placed last on the deck to terminate the program. The program is designed to run on the regular monitor operation service, but for runs longer than 15 minutes (the operation service limit) the program must be run individually. Three tapes are required, in addition to the Fortran 60 compiler tape, to run the program on the 1604 computer. These tapes are the input, output, and graph plot tapes.

(To perform runs without the graph plotter pull the "call graph card", the title cards (4 thru 9), and the card that "reads in" the title card.

thesL44

Computer simulation studies of copper at



3 2768 002 12022 2

DUDLEY KNOX LIBRARY